Are dipolar liquids ferroelectric?

David P. Shelton[a)]
Department of Physics, University of Nevada Las Vegas, Las Vegas, Nevada 89154-4002

(Received 3 May 2005; accepted 24 June 2005; published online 26 August 2005)

VH and HV depolarized hyper-Rayleigh scattering spectra were measured for liquid solutions of dipolar CH_3CN in nondipolar C_2Cl_4 at $T=300$ K. The VH spectrum contains a strong narrow peak due to a slowly relaxing longitudinal orientation mode. This peak is absent in the HV spectrum, and it disappears from the VH spectrum when the CH_3CN concentration is reduced to 8%. This observation is consistent with a ferroelectric phase transition predicted to occur when $\rho\mu_0^2 = 9\varepsilon_0 kT = 49$ D^2 M. © *2005 American Institute of Physics*. [DOI: 10.1063/1.2001643]

INTRODUCTION

Molecular reorientation in a normal liquid composed of small molecules occurs on the picosecond time scale, and the orientational fluctuations of anisotropic molecules scatter depolarized light with a typical spectral width of a few cm^{-1}. There is a long history of studies of molecular reorientation using depolarized Rayleigh scattering,[1–4] and more recently, sensitive time domain techniques have also been developed to study molecular motion.[5–8] These new techniques measure the sample response function instead of the spontaneous fluctuations, but give essentially the same information. In contrast, second-harmonic or hyper-Rayleigh scattering (HRS) measures spontaneous fluctuations and gives access to information which is inaccessible to Rayleigh scattering.[9–12]

The present work is motivated by the results of recent HRS spectral measurements for liquid water.[13,14] Those measurements were made in the usual 90° scattering geometry with linearly polarized light, for which one may define one polarized intensity I_{VV} and three depolarized intensities I_{HV}, I_{VH}, and I_{HH}, where the first and second subscripts refer to the vertical (V) or horizontal (H) linear polarizations of the incident and scattered light with respect to the horizontal scattering plane, respectively. The HV and VH depolarized spectra, which must be identical by symmetry when studied by depolarized Rayleigh scattering, were found to be different when measured by HRS, and the VH spectrum was found to contain a narrow unresolved peak due to a longitudinal collective mode.[13] Subsequent higher-resolution measurements put an upper bound of 6 MHz (0.0002 cm^{-1}) on the full width at half maximum (FWHM) intensity of the narrow VH component.[14] This corresponds to relaxation on a time scale longer than 50 ns, an unexpectedly long time for reorientation of water molecules in room-temperature liquid water.

Slow reorientation of small molecules can result from collective motion of the molecules such as occurs in liquid crystals, and a possible explanation for the slow relaxation observed in liquid water is the presence of domains of ferroelectric order. The simplest mean-field model of a dipolar medium gives the macroscopic polarization due to alignment of the molecular dipoles as $P=\rho\mu_0\langle\cos\theta\rangle$, where ρ is the molecular number density, μ_0 is the molecular dipole moment, $\langle\cos\theta\rangle=\mu_0 E_{loc}/3k_BT$ is the degree of alignment of the dipoles along the field direction, and $E_{loc}=E+P/3\varepsilon_0$ is the Lorentz local field. Combining these expressions gives $P=(\rho\mu_0^2 E/3k_BT)/(1-\rho\mu_0^2/9\varepsilon_0 k_BT)$, which diverges at $\rho\mu_0^2 = 9\varepsilon_0 k_BT = 49$ D^2 M for $T=300$ K. This simple model predicts that a ferroelectric phase transition will occur, and a macroscopic polarization will appear when $\rho\mu_0^2$ is above the threshold value $9\varepsilon_0 k_BT$. This threshold is exceeded for many polar liquids, for example, $\rho\mu_0^2$ (D^2 M)=293 for acetonitrile, 190 for water, 113 for acetone, and 71 for methanol.[15] This calculation predicting a "polarization catastrophe" is well known, and the observed absence of spontaneous macroscopic polarization in dipolar liquids is usually taken as evidence for the failure of the Lorentz local-field model. However, the observed absence of spontaneous macroscopic polarization may instead be due to the formation of microscopic ferroelectric domains which slowly relax or reorient.

This experiment is intended to test the idea of ferroelectric domains in liquids. If they are present there should be a threshold molecular dipole moment density for the appearance of the ferroelectric phase, and when the dipolar molecules are sufficiently diluted with nondipolar molecules the ferroelectric phase responsible for the slow relaxation and narrow VH peak should disappear. In this study we have chosen acetonitrile (CH_3CN) rather than water as the dipolar molecule. The depolarized spectrum is wider for acetonitrile, making it easier to distinguish the narrow VH component despite the limited resolution of the available grating spectrometer, and there are no hydrogen bond interactions between molecules to complicate the interpretation of the results. The acetonitrile is diluted with tetrachloroethylene (C_2Cl_4), a centrosymmetric molecule with no dipole moment and no allowed HRS spectrum. These two liquids are miscible in all proportions for temperatures above the 13 °C upper critical solution temperature.[16]

The outline for this paper is as follows. First, linear and nonlinear light-scattering techniques are compared, then the experiment and results are described, and finally the evidence for the idea of ferroelectric domains in dipolar liquids is discussed.

[a)]Electronic mail: shelton@physics.unlv.edu

COMPARISON OF LIGHT-SCATTERING PROBES OF LIQUIDS

Although the light wavelength is much longer than the molecular scale, inelastic and quasielastic light scattering are very useful probes of molecular dynamics in liquids because molecular motion results in scattered light fluctuations and frequency shifts which are readily observed in the time domain or the frequency domain.[1–3] The light scattered due to density fluctuations has the same polarization as the incident light, whereas light scattered by orientational fluctuations of anisotropic molecules is depolarized. Therefore, polarization analysis of the scattered light allows one to selectively probe either density fluctuations or orientational motion of the molecules. Since the instantaneous light signal seen by the detector is the sum of the scattered fields from all the molecules in the sample volume, the signal is sensitive to collective motion of the molecules. The linear light-scattering spectrum is determined by the time correlation function of the molecular polarizability tensor $\boldsymbol{\alpha}$:

$$\langle E_\varepsilon(t)E_\varepsilon(t+\tau)\rangle \propto \Sigma_{\alpha,\beta}E_\alpha E_\beta\langle\Sigma_{a,b}\alpha_{\varepsilon\alpha}(\mathbf{r}_a,\boldsymbol{\Omega}_a,t) \times\alpha_{\varepsilon\beta}(\mathbf{r}'_b,\boldsymbol{\Omega}'_b,t+\tau)\cos(\Delta\mathbf{k}\cdot\mathbf{r}_{ab})\rangle, \quad (1)$$

where $\langle\ \rangle$ is the time average, $\mathbf{r}_a,\boldsymbol{\Omega}_a(\mathbf{r}'_b,\boldsymbol{\Omega}'_b)$ is the position and orientation of molecule a (b) at time $t(t+\tau)$, $\Delta\mathbf{k}=\mathbf{k}_i-\mathbf{k}_s$ is the scattering wave vector, $\mathbf{k}_i$ ($\mathbf{k}_s$) is the wave vector of the incident (scattered) photon, $\mathbf{r}_{ab}=\mathbf{r}_a-\mathbf{r}'_b$ is the relative position vector, and a and b are both summed over all N molecules in the sample volume. E_α and E_β are Cartesian components of the linearly polarized incident light field, E_ε is the ε polarized component of the scattered field, and $\alpha_{\varepsilon\alpha}$ are laboratory-frame Cartesian components of $\boldsymbol{\alpha}$. The spectral intensity is the Fourier transform of the time correlation function $\langle E_\varepsilon(t)E_\varepsilon(t+\tau)\rangle$. If the motions of the different molecules are completely uncorrelated, the correlation function reduces to just the incoherent sum of the single molecule correlation functions: $N\langle\boldsymbol{\alpha}(\mathbf{r}_a,\boldsymbol{\Omega}_a,t)\boldsymbol{\alpha}(\mathbf{r}'_a,\boldsymbol{\Omega}'_a,t+\tau)\rangle$.

The time scales of molecular motions in normal liquids typically result in a scattered light spectrum with frequency shifts in the range of 0.1–100 cm^{-1}. Molecular reorientation in liquids composed of small molecules typically occurs on the picosecond time scale and gives a spectral width of a few cm^{-1}. Very localized density fluctuations occur on the $<$0.1-ps intermolecular collision time scale and give spectral widths of 10–100 cm^{-1}, whereas long-range density fluctuations occur on the $>$100-ps time scale and give a spectral width of $<$0.1 cm^{-1}. The long-range density fluctuations result in the Rayleigh-Brillouin spectrum. The unshifted central Rayleigh peak is associated with diffusively dissipated density fluctuations, while the Brillouin doublet is due to propagating sound waves. As the liquid is cooled the viscosity increases, relaxations slow, and additional spectral features appear. The Mountain peak due to structural relaxation appears in the polarized spectrum, and the central Rytov dip in the depolarized spectrum due to translation-rotation coupling evolves into a pair of Brillouin peaks due to shear waves. The same liquid dynamics can also be probed by time domain techniques such as photon correlation spectroscopy (PCS),[1,3] impulsive stimulated light scattering (ISS),[6,7] and optical-heterodyne-detected optical Kerr effect (OHD-OKE).[5,8] In PCS the autocorrelation function of spontaneous intensity fluctuations is measured. In the latter two techniques a pump beam induces a spatial grating or refractive index anisotropy, the decay of which is read out by a probe beam. These techniques measure the sample response function, which is related to spontaneous fluctuations by the fluctuation-dissipation theorem. Although essentially the same information is in principle available to frequency and time domain measurements, time domain measurements have the advantage for slow and complex relaxations, and where a wide range of time scales must be probed.

Second harmonic or HRS is a nonlinear optical technique that also probes the collective reorientation dynamics in molecular liquids.[9–13] The scattered light intensity at the second harmonic of the incident frequency is determined by the time correlation function of the third rank molecular hyperpolarizability tensor $\boldsymbol{\beta}$:

$$\langle E_\varepsilon(t)E_\varepsilon(t+\tau)\rangle \propto \Sigma_{\alpha,\beta,\gamma,\delta}E_\alpha E_\beta E_\gamma E_\delta\langle\Sigma_{a,b}\beta_{\varepsilon\alpha\beta}(\mathbf{r}_a,\boldsymbol{\Omega}_a,t) \times\beta_{\varepsilon\gamma\delta}(\mathbf{r}'_b,\boldsymbol{\Omega}'_b,t+\tau)\cos(\Delta\mathbf{k}\cdot\mathbf{r}_{ab})\rangle, \quad (2)$$

analogous to Eq. (1), with $\Delta\mathbf{k}=2\mathbf{k}_i-\mathbf{k}_s$. However, by symmetry, HRS gives access to information complementary to that obtained from linear light scattering. Consider the effect of orientational correlations of the molecules on the scattered intensity. Any molecular response tensor $\mathbf{A}$ can be decomposed into a direct sum of irreducible spherical tensors, and the scattered intensity obtained from Eq. (1) or Eq. (2) can be expressed as the sum of terms of the form $\langle\mathbf{A}_a^{[k]}\mathbf{A}_b^{[k]}\rangle$, where $\mathbf{A}_a^{[k]}$ is an irreducible spherical tensor of rank k associated with molecule a, and $\langle\ \rangle$ is the ensemble average over molecular orientations with distribution $G(\boldsymbol{\Omega}_a,\boldsymbol{\Omega}_b)$.[9,17] Two limiting forms for the pair orientational distribution function are (i) $G(\boldsymbol{\Omega}_a,\boldsymbol{\Omega}_b)=G(\boldsymbol{\Omega}_a-\boldsymbol{\Omega}_b)$, which gives intermolecular orientational correlation and laboratory-frame isotropy, and (ii) $G(\boldsymbol{\Omega}_a,\boldsymbol{\Omega}_b)=G(\boldsymbol{\Omega}_a)G(\boldsymbol{\Omega}_b)$, which gives orientational bias with respect to laboratory axes. Expanding the function $G(\boldsymbol{\Omega})$ as a sum of Wigner rotation matrices $D_{np}^{[m]}(\boldsymbol{\Omega})$,

$$G(\boldsymbol{\Omega})=\Sigma_{m,n,p}G_{np}^{[m]}D_{np}^{[m]}(\boldsymbol{\Omega}) \quad (3)$$

one may show that the zeroth rank component of $G(\boldsymbol{\Omega}_a,\boldsymbol{\Omega}_b)$ always gives a nonvanishing contribution for incoherent scattering (where $a=b$), but only the kth rank components of $G(\boldsymbol{\Omega}_a,\boldsymbol{\Omega}_b)$ give nonvanishing contributions to $\langle\mathbf{A}_a^{[k]}\mathbf{A}_b^{[k]}\rangle$ for cooperative scattering (where $a\neq b$). Since the irreducible decomposition of the nonresonant response tensors gives $\boldsymbol{\alpha}=\boldsymbol{\alpha}^{[0]}\oplus\boldsymbol{\alpha}^{[2]}$ and $\boldsymbol{\beta}=\boldsymbol{\beta}^{[1]}\oplus\boldsymbol{\beta}^{[3]}$, of even and odd ranks, respectively, one sees that orientational correlations of opposite parity contribute to cooperative light scattering mediated by $\boldsymbol{\alpha}$ and $\boldsymbol{\beta}$. In particular, HRS is sensitive to polar orientational order with a distribution of the form $D_{00}^{[1]}(\boldsymbol{\Omega})=\cos\theta$, whereas linear light scattering is not. Conversely, linear light scattering is sensitive to isotropic density fluctuations such as sound waves, where $D_{00}^{[0]}(\boldsymbol{\Omega})=1$, but HRS is not.

In the case of randomly oriented molecules the contributions from the individual molecules are summed incoherently to give the total Rayleigh or hyper-Rayleigh scattering intensity, and the three depolarized scattering intensities I_{HV}, I_{VH},

and I_{HH} for the usual 90° scattering geometry with linearly polarized light are identical by symmetry for both RS and HRS. Thus, the intensity ratio is $I_{HV}/I_{VH}=1$ for both RS and HRS in the case of randomly oriented molecules. The intensity ratio is also $I_{HV}/I_{VH}=1$ for both RS and HRS in the case of a distribution $D_{00}^{[2]}(\mathbf{\Omega})=(3\cos^2\theta-1)/2$ where the molecules are aligned along a laboratory-fixed direction. However, $I_{HV}/I_{VH}\neq 1$ for HRS in the case of a distribution $D_{00}^{[1]}(\mathbf{\Omega})=\cos\theta$ where the dipolar molecules are polarized along a laboratory-fixed direction. The ratio of depolarized HRS intensities is $I_{HV}/I_{VH}=0$ for the molecules polarized in the direction of the scattering vector $\Delta\boldsymbol{k}$ (longitudinal), and $I_{HV}/I_{VH}=2$ for the molecules polarized perpendicular to the scattering vector (transverse).[10,13,18] Therefore, HRS measurements probing fluctuations with wave vector $\Delta\boldsymbol{k}$ will distinguish between longitudinal and transverse polarized collective modes of an isotropic dipolar liquid.

Thus, HRS is sensitive to polar order of the molecules and distinguishes between isotropic, longitudinal and transverse fluctuations, whereas polar reorientation modes are invisible to RS. Information about polar collective modes is contained in the differences between the HV and VH depolarized HRS spectra.

HRS EXPERIMENT

The apparatus was the same as previously described,[13,19] except that the laser was injection seeded so that its output was in a single longitudinal mode. The beam from the pulsed neodymium: yttrium aluminum garnet (Nd:YAG) laser at $\lambda=1064$ nm was focused into the liquid sample contained in a 1-cm fused silica fluorimeter cuvette placed in a thermostatic enclosure at $T=27.0$ °C, and the scattered light near $\theta=90°$ and $\lambda=532$ nm was collected with a $f/1.8$ lens and analyzed by a grating spectrometer with calibrated spectral response. The incident beam in the sample had a waist diameter of 10 μm, and the pulses had a 2.2-kHz repetition rate, 90-ns duration, and 0.5–1-mJ energies. The reagent grade samples were filtered through a 0.2-μm micropore filter. The polarization of the incident laser beam was controlled using a prism polarizer and an electronically controlled liquid-crystal wave plate, while the polarization of the collected light was analyzed using a sheet polarizer mounted to allow the polarization axis to be rotated rapidly by 90°. Multiple VH and HV scans were alternated to eliminate bias due to drift in alignment. A liquid-crystal 45° rotator placed between the analyzing polarizer and the grating spectrometer equalized the response for H and V polarizations. The measured deviations from constant response were less than 5% for both polarizations over the 100-cm^{-1} spectral range used in this work. The measured spectra were corrected for the instrument response, but were not corrected for polarization mixing due to the finite collection angle.

Since the time-averaged laser linewidth was <0.01 cm^{-1}, the spectral resolution was entirely determined by the grating spectrometer. The 0.4-cm^{-1} spectral slit width (SSW) chosen for the high-resolution HRS spectra was the best compromise between the conflicting requirements for maximum signal throughput and maximum spectral resolution. With this slit width the maximum peak signal for the high-resolution HRS spectra was 1 count/s, and the instrumental line shape was approximated well by the triangle function expected when operating far from the diffraction limit. The second-harmonic light generated by a potassium titanly phosphate (KTP) crystal was used to measure the instrumental line shape, and also as a marker for zero frequency shift. The 1.0×10^{-3}-count/s background due to the gated photomultiplier tube dark count rate was much smaller than the HRS signal.

The full available laser power was used in the case of neat acetonitrile. However, with average power about 2 W for the laser beam in the acetonitrile sample, thermal defocusing of the laser beam due to weak vibrational overtone absorption by CH_3CN molecules will cause a decrease in the HRS signal by about 10% or more. The measured HRS intensities in this work do not take into account the effect of this thermal lensing. The laser power was reduced to 1 W in the case of neat tetrachloroethylene and solutions with acetonitrile. Samples containing C_2Cl_4 have a tendency to self-destruct when exposed to a more powerful laser beam, due to the low thermal decomposition temperature of the C_2Cl_4. Although there is negligible absorption of the laser beam by C_2Cl_4, the hot spot formed if an absorbing dust particle passes through the laser beam focus can decompose some of the C_2Cl_4 and deposit a thin absorbing layer on the cell window. Then the laser beam absorption at the hot spot on the window where the absorbing layer is illuminated by the laser beam grows at an increasing rate due to thermal decomposition of the adjacent C_2Cl_4, and thermal decomposition eventually destroys the entire sample.

SPECTRAL RESULTS AND ANALYSIS

Figure 1 shows the VH and HV depolarized HRS spectra measured over a 10-cm^{-1} interval with 0.4-cm^{-1} resolution, for samples at $T=27.0$ °C with four different acetonitrile concentrations. Intensity is plotted as a function of frequency shift ν from the second harmonic of the laser (the Stokes side of the spectrum is shown with negative frequency shift). Each spectrum is the sum of 352–531 scans of 4-min duration. To make the spectra shown in Fig. 1 directly comparable, the plotted signals have been scaled to the values that would be observed with the same number of scans and a common value $P=1$ W for the laser beam power. The background due to the gated dark count rate of the detector is <0.5 count/channel in all these spectra. These HRS spectra evolve in a complicated way as the acetonitrile is diluted with tetrachloroethylene, so additional complementary measurements were made to help constrain the spectral fits and aid their interpretation. Information about the broad HRS spectral components underlying the narrower peaks in Fig. 1 is obtained from the HRS spectra measured over a wider 100-
cm^{-1} interval, with HV polarization and 4-cm^{-1} resolution, as shown in Fig. 2. The broad HRS spectral component is due to the molecular interactions during collisions and is identical for HV and VH polarizations. Additional information on molecular reorientation is obtained from the depolar-

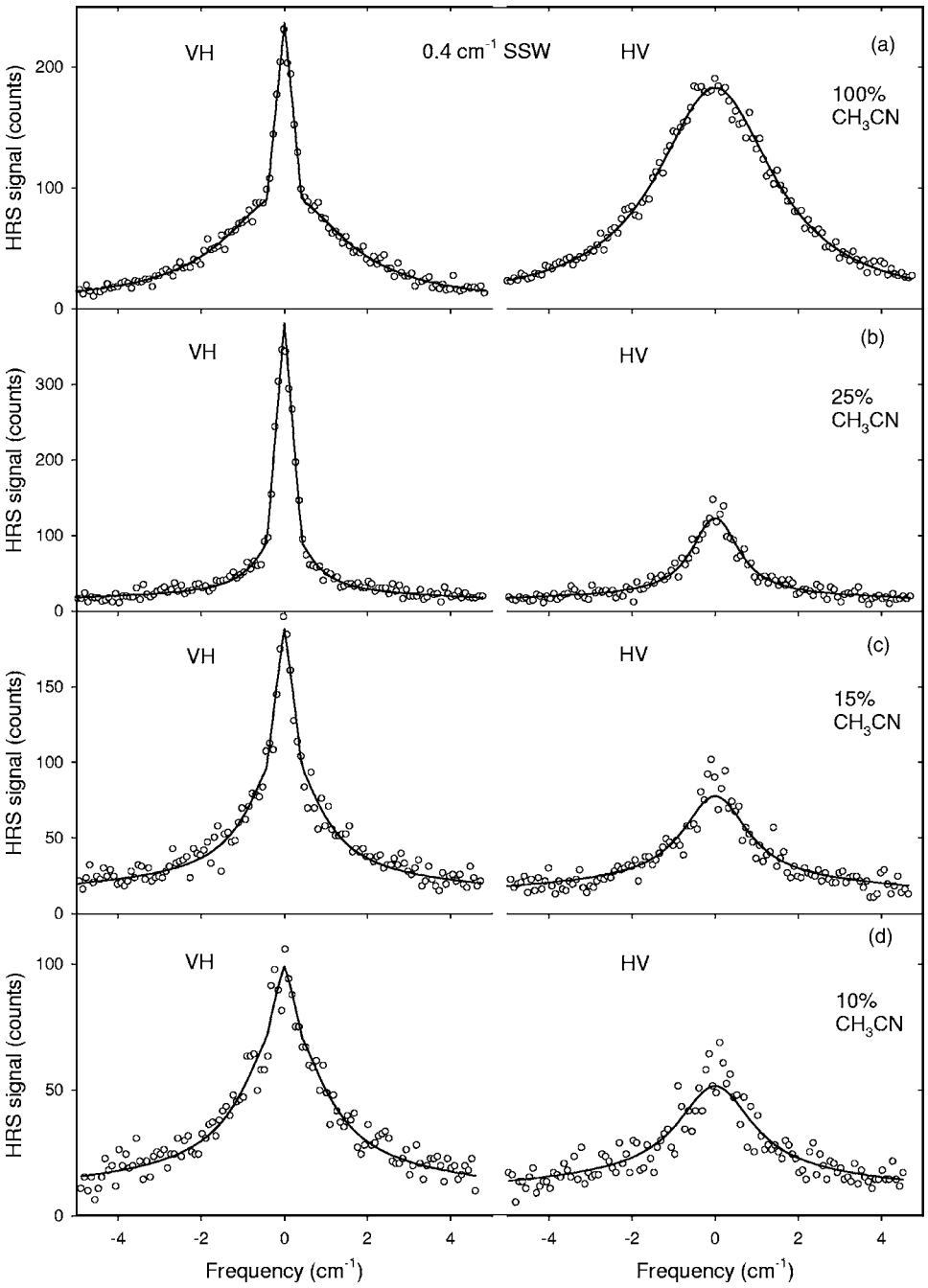

FIG. 1. HRS signal plotted vs frequency shift for four different liquid acetonitrile solutions at $T=27.0\,^{\circ}\mathrm{C}$. The spectra in each panel were obtained by alternating VH and HV scans [352, 448, 448, and 531 scans each in panels (a), (b), (c), and (d), respectively] and were corrected and normalized as stated in the text. The curves are the best fits to the spectra. The sharp triangular peaks in the VH spectra are instrumentally broadened.

ized HV Rayleigh scattering spectra shown in Fig. 3, which are measured over 10- and 100-cm^{-1} intervals for CH_3CN and C_2Cl_4, using a 2-mW continuous single longitudinal-mode laser beam at 532 nm for excitation. Due to the large solid angle for the collection optics there is some leakage of the intense VV polarized Rayleigh scattering into the HV Rayleigh spectra, and this is visible as a small sharp bump at zero frequency in the acetonitrile spectra in Fig. 3.

The analysis of these spectra is modeled on the analysis of the HRS spectra previously measured for water.[13] They are represented as the sum of three distinct components: a Lorentzian spectral function $f_L(\nu,w_L)=[1+(\nu/w_L)^2]^{-1}$ due to transverse and isotropic reorientations, a broad spectral component $f_B(\nu)$ due to short-duration intermolecular collisions, and a spectrally unresolved peak due to slow longitudinal reorientation. The HRS spectra for mixtures of acetonitrile and tetrachloroethylene in Fig. 1 are assumed to have the form

$$I_{\mathrm{HV}}(\nu)=A_{\mathrm{HV}}f_L(\nu,w_L)+Bf_B(\nu), \tag{4a}$$

$$I_{\mathrm{VH}}(\nu)=A_{\mathrm{VH}}f_L(\nu,w_L)+Bf_B(\nu)+C\delta(\nu), \tag{4b}$$

where the fit parameters are the width w_L and the intensity coefficients A_{VH}, A_{HV}, B, and C, and where the shape of the low, broad component $f_B(\nu)$ is determined from fits to the spectra in Fig. 2. The functions in Eqs. (4) are multiplied by the instrumental response function (accounting for frequency dependence of the instrument frequency bandpass, transmission, and detection efficiency), multiplied by the factor $(\nu_s/\nu_0)^3\exp(-hc\nu/2kT)$, where ν_s and ν_0 are the scattered

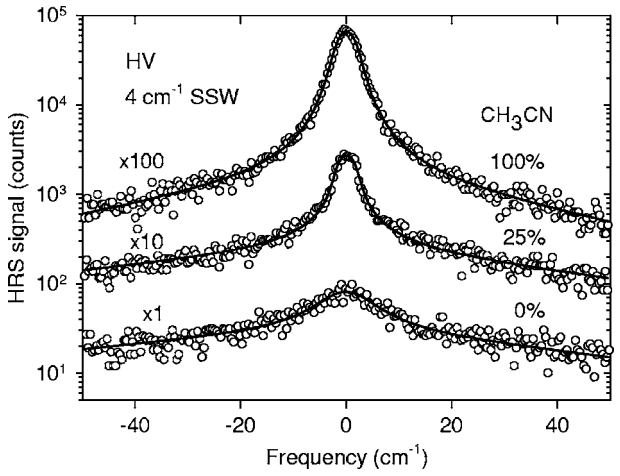

FIG. 2. HRS signal plotted vs frequency shift over a wide scan range for three mixtures of acetonitrile and tetrachloroethylene at $T=27.0\,^{\circ}\mathrm{C}$. The successive spectra are offset for clarity, and the curves are best fits to the spectra. The collision-induced contribution dominates at large frequency shift.

and incident light frequencies, added to the detector background, convolved with the triangular instrument function $[f_T(\nu,w_T)=1-|\nu/w_T|$ for $|\nu/w_T|<1$, otherwise 0], and jointly fitted to the VH and HV spectral pairs measured for each sample. The values of χ^2 for these fits, calculated assuming the error bars determined by counting statistics alone, are in the range of $208<\chi^2<242$, which is not significantly different from the expected value $\chi^2=230\pm21$ predicted from the number of degrees of freedom for the fit. The fit parameters are only weakly interdependent and are insensitive to the shape of the broad component. The results of these fits are given in Table I and shown as the curves in Fig. 1.

A similar fitting procedure is used to obtain the shape of the broad HRS component $f_B(\nu)$ from the spectra in Fig. 2. The collision-induced spectrum is expected to have an exponential form $f_E(\nu,w_E)=\exp[-|\nu/w_E|]$. However, an adequate fit to the HRS spectrum for tetrachloroethylene, which is purely collision induced, requires the sum of a broad Lorentzian function and an exponential function. The collision-induced spectrum for neat acetonitrile is relatively weak, and in this case the HV HRS spectrum is adequately fitted by just the sum of a single Lorentzian for the allowed orientational spectrum and a single exponential for the collision-induced spectrum. For mixtures, the broad component $f_B(\nu)$ is adequately represented by the following linear combination of the collision-induced spectrum for acetonitrile (first term) and the collision-induced spectrum for tetrachloroethylene (last two terms):

$$f_B(\nu)=B_1f_E(\nu,w_1)+B_2f_L(\nu,w_2)+B_3f_E(\nu,w_3). \tag{5}$$

The function $f_B(\nu)$ is normalized and the coefficients obey $B_1+B_2+B_3=1$. The fits to the spectra in Fig. 2 give relations $B_1/B_2=(0.34\pm0.04)y/(1-y)$ and $B_3/B_2=0.64\pm0.08$ for the coefficients, where y is the volume fraction of acetonitrile in the solution, and $w_1=35\pm3$ cm^{-1}, $w_2=6.1\pm0.7$ cm^{-1}, and $w_3=69\pm13$ cm^{-1} for the widths. The fits in Fig. 1 assume these results for $f_B(\nu)$.

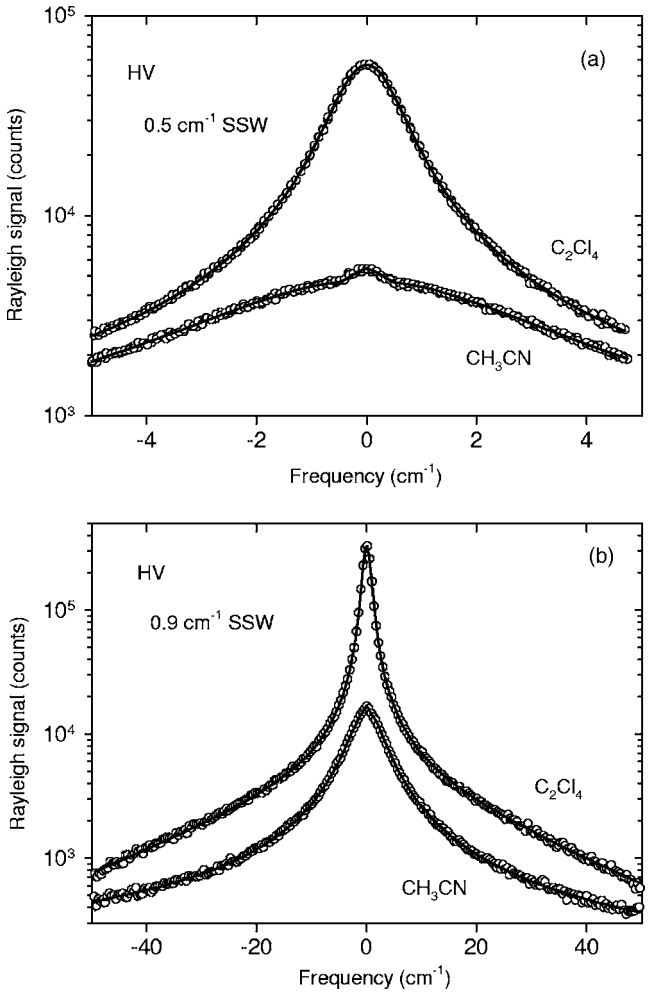

FIG. 3. Depolarized Rayleigh signal plotted vs frequency shift for liquid acetonitrile and tetrachloroethylene at $T=27.0\,^{\circ}\mathrm{C}$, for (a) narrow and (b) wide scans. The curves are best fits to the spectra. The small triangular bumps visible at 0 cm^{-1} in the acetonitrile spectra are due to leakage of VV scattered light.

The HV Rayleigh spectra in Fig. 3 are fitted assuming that they are each the sum of two Lorentzians, one exponential, and a delta function due to the VV light leak. For acetonitrile the fitted curves are within the error bars given by

TABLE I. Fit parameters for the VH and HV HRS spectra in Fig. 1, using the functions in Eqs. (4). Peak heights A, B, C/w_T and integrated intensities I are normalized to the HV Lorentzian component for 100% CH$_3$CN, which is the best determined component. The instrumentally broadened triangular spike in the VH spectrum has peak height C/w_T and width $w_T=0.42$ cm^{-1}.

CH$_3$CN concentration	100%	25%	15%	10%
A_{HV}	1	0.61±0.03	0.32±0.02	0.20±0.01
A_{VH}	0.49±0.01	0.54±0.03	0.49±0.03	0.34±0.02
B	0.031±0.004	0.117±0.004	0.120±0.005	0.090±0.005
C/w_T	0.79±0.03	1.49±0.08	0.43±0.06	0.11±0.05
$I_{A\mathrm{HV}}$	1	0.22±0.01	0.17±0.01	0.12±0.01
$I_{A\mathrm{VH}}$	0.49±0.01	0.20±0.01	0.26±0.02	0.21±0.01
I_B	0.42±0.06	1.45±0.05	1.49±0.06	1.11±0.06
I_C	0.062±0.002	0.117±0.006	0.034±0.005	0.009±0.004
w_L (cm^{-1})	1.68±0.03	0.62±0.03	0.90±0.06	1.04±0.08

TABLE II. Fit parameters for HV Rayleigh spectra in Fig. 3. Peak height and integrated intensity are normalized to the narrow Lorentzian component for CH_3CN.

Liquid	Spectral component	Width (cm^{-1})	Peak height	Integrated intensity
CH_3CN	*L*1	3.39±0.05	1	1
	*L*2	11.6±1.5	0.108±0.009	1.25±0.19
	*E*1	80±16	0.038±0.006	3.0±0.8
C_2Cl_4	*L*1	0.65±0.05	13.6±0.2	2.53±0.05
	*L*2	2.8±0.4	0.71±0.12	2.0±0.3
	*E*1	21.2±0.4	0.25±0.03	5.3±0.5

counting statistics. For tetrachloroethylene the fit is also close, although in this case the statistical error bars are very narrow and χ^2 indicates statistically significant discrepancies. The results are given in Table II. Note that the reorientation spectrum for tetrachloroethylene is very strong in RS due to the large molecular polarizability anisotropy, but is forbidden in HRS since the molecule is centrosymmetric. The polarizabililty of tetrachloroethylene is much larger than that of acetonitrile, while the quadrupole moments are nearly the same.[15,20]

A comparison of the HRS and Rayleigh spectral fit results in Tables I and II shows that the widths of the narrow Lorentzian components in the HV HRS and RS spectra of neat acetonitrile differ by a factor of 2, somewhat less than the factor 3 one would expect for anisotropic molecules undergoing rotational diffusion. The narrow Lorentzian component in the RS spectrum for tetrachloroethylene is five times narrower than for acetonitrile, which indicates that reorientation of tetrachloroethylene is five times slower. Combining these results, one can understand the narrowing of the HV HRS spectrum for the mixtures as due to slower reorientation of acetonitrile molecules in the presence of slowly reorienting neighboring tetrachloroethylene molecules, and one can estimate that a Lorentzian component with width $w_L = 0.33\ cm^{-1}$ would appear in the HRS spectrum if the acetonitrile molecules reoriented at the same rate as the surrounding tetrachloroethylene molecules. The observed width is as small as $0.62\ cm^{-1}$, which indicates that the acetonitrile molecules in solution reorient at least twice as fast as the tetrachloroethylene molecules.

The widths of the broad components in the HRS and RS spectra are quite different, which is understandable since collision-induced contributions can occur through dipole-induced-dipole, quadrupole-induced-dipole, and many higher-order interactions. These interactions have different dynamics and contribute in different proportions to HRS and Rayleigh scattering. The HRS intensity ratio $I_{VV}/I_{HV} = 3.5 \pm 0.2$ measured for neat tetrachloroethylene carries some information about the interaction mechanism.[21]

The polarization dependence of the HRS spectral components allows one to classify them. Consider longitudinal and transverse collective modes of molecular orientation, of the same amplitude and with the wave vector picked out by the scattering process. The VH HRS intensities will be the same for these two modes, but the HV HRS intensity will be twice as large as the VH HRS intensity for the transverse mode, and zero for the longitudinal mode.[13,18] Considering the polarization dependence of the HRS spectrum of neat acetonitrile shows that it is relatively simple. In neat acetonitrile the Lorentzian component is twice as intense in HV as in VH, which identifies it as a nearly pure transverse mode. The narrow spike is present only in the VH spectrum, which identifies it as a longitudinal mode. The broad spectral component is due to isotropic collision-induced fluctuations and has the same intensity for HV and VH polarizations. Based on the integrated intensities of the components in the HV spectrum, the transverse mode is eight times stronger than the longitudinal mode. The relaxation times for the transverse and longitudinal modes are distinct and very different in neat acetonitrile.

When the acetonitrile is diluted with tetrachloroethylene the width of the Lorentzian component decreases and the VH spectrum becomes more intense than the HV spectrum. The narrow spike is most prominent in the 25% acetonitrile spectrum and must still be due to a slowly relaxing longitudinal mode since it only appears in the VH spectrum, but the intensity ratio I_{HV}/I_{VH} for the Lorentzian component is now consistent with some indeterminate mixture of isotropic, transverse and longitudinal modes all with the same relaxation time. At the acetonitrile concentration of 10%, where the narrow spike has nearly disappeared and the Lorentzian component is 1.7 times more intense for VH than for HV, the longitudinal-mode strength must be at least 3.5 times greater than the transverse-mode strength.

DISCUSSION AND CONCLUSION

The outstanding observation in this work is the presence of a narrow spike in the VH HRS spectrum. The true width of the spike observed for acetonitrile solutions is much smaller than the $0.4\text{-}cm^{-1}$ instrumental resolution and is thought to be similar to the $0.0002\text{-}cm^{-1}$ width measured for the corresponding peak in water.[14] This feature is attributed to slowly reorienting ferroelectric domains which are expected to disappear when the concentration of dipolar molecules in the liquid falls below some threshold concentrations. The narrow spike is certainly present for 15% acetonitrile concentration and higher since the 15% acetonitrile spectrum cannot be adequately fitted with the spike set to zero. The spike is much weaker in the 10% solution, and a fit with the spike height set to zero for the 10% solution is not significantly worse than the best fit which includes the spike height as a free parameter. Figure 4 shows the height of the narrow triangular spike in the VH HRS spectrum plotted as a function of acetonitrile concentration. This graph is the main result of this work, and it shows that the height of the spike falls rapidly to zero near 10% acetonitrile concentration.

A ferroelectric transition is predicted to occur when the dipole moment density exceeds the threshold value $\rho\mu_0^2 = 9\varepsilon_0 k_B T = 49\ D^2\ M$ for $T = 300$ K. The threshold acetonitrile concentration for the ferroelectric transition may be estimated based on the concentration $\rho = 19.1M$ for neat liquid acetonitrile and the gas-phase value $\mu_0 = 3.92$ D for the dipole moment of acetonitrile.[15] Thus one obtains $\rho\mu_0^2$

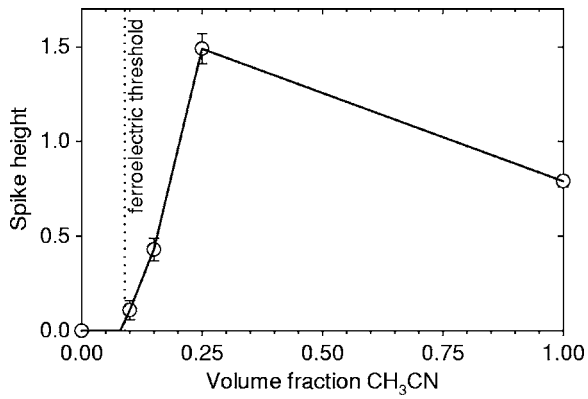

FIG. 4. Height of the narrow spike in the VH HRS spectrum (C/w_T from Table I) plotted vs acetonitrile concentration. The vertical dotted line marks the predicted ferroelectric threshold and the solid line joins the data points as a guide to the eye.

$=293\ \mathrm{D}^2\,\mathrm{M}$ for neat liquid acetonitrile and predicts that the threshold value $\rho\mu_0^2=49\ \mathrm{D}^2\,\mathrm{M}$ will be reached for a 17% acetonitrile solution. However, the dipole moment of an acetonitrile molecule is altered when it is placed in a polarizable environment such as liquid tetrachloroethylene solution, and this effect should be included when predicting the threshold concentration. A polarizable dipolar molecule may be represented as a dielectric sphere with permanent moment μ_0 and dielectric constant $\varepsilon_1=n_1^2$ embedded in a dielectric continuum with dielectric constant $\varepsilon_2=n_2^2$, where n is the refractive index.[22,23] The field in the dielectric outside the sphere is the same as that of a point dipole with value μ given by

$$\mu=\mu_0\frac{n_1^2+2}{(n_1/n_2)^2+2}. \tag{6}$$

The refractive indices are $n_1=1.34$ for acetonitrile and $n_2=1.50$ for tetrachloroethylene.[15] The dipole moment obtained from Eq. (6) for neat liquid acetonitrile is 8% higher than the dipole moment calculated for an acetonitrile molecule in a cluster with liquid structure.[24] The dipole moment given by Eq. (6) for acetonitrile dissolved in tetrachloroethylene is 1.36 times larger than the gas-phase value, and the corresponding ferroelectric transition threshold is predicted to occur at 9% acetonitrile concentration. Figure 4 shows that the experimentally determined spike height vanishes at about 8% acetonitrile concentration, in good agreement with the predicted threshold concentration for the ferroelectric transition. This is taken as evidence for the existence of ferroelectric domains.

The polar order parameter for the ferroelectric domains may be estimated from HRS intensity measurements combined with an estimate of the size of the domains. Although the domain size is unknown, a domain size of the order of 10 nm is plausible since collective reorientation of the molecules in such a domain would be several orders of magnitude slower than rotational diffusion of individual molecules and so could account for a relaxation time comparable to the slow relaxation time observed for water. The intensity of coherent scattering from M molecules with polar order parameter $g=\langle\cos\theta\rangle$, within a correlation volume ξ^3 in a fluid of number density ρ, is $Mg^2=\rho\xi^3g^2$ times as large as the incoherent scattering intensity from the same M molecules randomly oriented. In the small order parameter limit this gives $g=\rho^{-1/2}\xi^{-3/2}\,[I(\mathrm{coherent})/I(\mathrm{incoherent})]^{1/2}$. Estimating that the integrated intensities of the coherent and incoherent contributions to the orientational HRS spectrum are approximately equal for the 25% acetonitrile solution and setting $\rho=0.25\times19.1\mathrm{M}$ and $\xi=10$ nm gives $M=3\times10^3$ and $g=2\times10^{-2}$, with corresponding intradomain field $E=P/3\varepsilon_0=g\rho\mu/3\varepsilon_0=40$ MV/m. The estimated value of the polar order parameter is small.

Liquids composed of dipolar molecules pose an especially difficult theoretical problem due to the complication of an infinite range interaction whose sign is dependent on the relative orientation of the molecules. Theory predicts a rich variety of structures and dynamic collective effects for model dipolar liquids,[25–45] but most theoretical results and simulations have been obtained for systems of small size, with simplified interactions and without dynamics. At low density, dipolar hard or soft spheres tend to form chains,[28,34] and at high density a ferroelectric fluid phase is predicted.[29,42] The ferroelectric phase for the strongly coupled model dipolar fluid[29,30,32,34,37,42] is inhomogenously polarized with a vortex structure and thick domain walls,[34] rather different from the domains of ferroelectric and ferromagnetic crystalline solids. The results for dipolar fluids appear to be in contrast to the results for dilute dipole impurities in insulating crystals, which indicate that destruction of long-range ferroelectric order results from the large fluctuations of the local field, and that long-range ferroelectric order is not possible for disordered systems with purely dipolar interactions unless the host crystal is highly polarizable.[45] However, a recent *ab initio* simulation of ferroelectric crystalline $Pb(Zr,Ti)O_3$ (PZT) nanoparticles finds phases with toroidal ordering of the dipole moments resembling the molecular orientations in smectic or cholesteric liquid crystals.[46] In this case there is no net polarization of the domains despite strong ordering of the dipole moments. A similar large vortexlike structure of the dipole field is also found in a recent molecular-dynamics simulation of liquid water.[47]

In conclusion, the experimental evidence presented here for ferroelectric structure in dipolar liquids is the observation of a slowly relaxing longitudinal polar mode which disappears at the predicted ferroelectric threshold. The present experimental observations are consistent with the results of theoretical calculations and simulations which suggest that the ferroelectric phase of a dipolar liquid will have domains with a vortexlike structure and a small value for the polar order parameter.

[1] B. J. Berne and R. Pecora, *Dynamic Light Scattering* (Wiley, New York, 1976).
[2] D. Kivelson and P. A. Madden, Annu. Rev. Phys. Chem. **31**, 523 (1980).
[3] G. D. Patterson and P. J. Carroll, J. Phys. Chem. **89**, 1344 (1985).
[4] S. Takagi and H. Tanaka, Phys. Rev. Lett. **93**, 257802 (2004).
[5] Y. J. Chang and E. W. Castner, J. Chem. Phys. **99**, 113 (1993).
[6] Y. Yang and K. A. Nelson, J. Chem. Phys. **103**, 7722 (1995).
[7] C. Glorieux, K. A. Nelson, G. Hinze, and M. D. Fayer, J. Chem. Phys. **116**, 3384 (2002).
[8] H. Cang, J. Li, N. Novikov, and M. D. Fayer, J. Chem. Phys. **118**, 9303 (2003).

[9] P. D. Maker, Phys. Rev. A **1**, 923 (1970).
[10] V. N. Denisov, B. N. Mavrin, and V. B. Podobedov, Phys. Rep. **151**, 1 (1987).
[11] K. Clays and A. Persoons, Phys. Rev. Lett. **66**, 2980 (1991).
[12] D. P. Shelton and P. Kaatz, Phys. Rev. Lett. **84**, 1224 (2000).
[13] D. P. Shelton, J. Chem. Phys. **117**, 9374 (2002); **121**, 3349(E) (2004).
[14] D. P. Shelton, Phys. Rev. B **72**, 020201 (2005).
[15] R. C. Weast, *CRC Handbook of Chemistry and Physics*, 68th ed. (CRC, Boca Raton, 1987).
[16] IUPAC-NIST Solubility Database, srdata.nist.gov/solubility/sol_main_search.asp
[17] J. Jerphagnon, D. Chemla, and R. Bonneville, Adv. Phys. **27**, 609 (1978).
[18] D. P. Shelton, J. Opt. Soc. Am. B **17**, 2032 (2000).
[19] P. Kaatz and D. P. Shelton, Rev. Sci. Instrum. **67**, 1438 (1996).
[20] L. Reynolds, J. A. Gardecki, S. V. J. Frankland, M. L. Horng, and M. Maroncelli, J. Phys. Chem. **100**, 10337 (1996).
[21] S. Kielich, J. R. Lalanne, and F. B. Martin, Phys. Rev. Lett. **26**, 1295 (1971).
[22] H. Frolich, *Theory of Dielectrics*, 2nd ed. (Clarendon, Oxford, 1958).
[23] C. J. F. Bottcher and P. Bordewijk, *Theory of Electric Polarization*, 2nd ed. (Elsevier, Amsterdam, 1978), Vols. I and II.
[24] R. Rivelino, B. J. Costa Cabral, K. Coutinho, and S. Canuto, Chem. Phys. Lett. **407**, 13 (2005).
[25] N. H. March and M. P. Tosi, *Atomic Dynamics in Liquids* (Dover, New York, 1976).
[26] E. L. Pollock and B. J. Alder, Phys. Rev. Lett. **46**, 950 (1981).
[27] P. G. Kusalik, J. Chem. Phys. **93**, 3520 (1990).
[28] J. J. Weis and D. Levesque, Phys. Rev. Lett. **71**, 2729 (1993).
[29] J. J. Weis and D. Levesque, Phys. Rev. E **48**, 3728 (1993).
[30] D. Levesque and J. J. Weis, Phys. Rev. E **49**, 5131 (1994).
[31] M. J. Stevens and G. S. Grest, Phys. Rev. E **51**, 5962 (1995).
[32] B. Groh and S. Dietrich, Phys. Rev. E **53**, 2509 (1996).
[33] S. Ravichandran and B. Bagchi, Phys. Rev. E **54**, 3693 (1996).
[34] B. Groh and S. Dietrich, Phys. Rev. Lett. **79**, 749 (1997).
[35] B. Groh and S. Dietrich, Phys. Rev. E **55**, 2892 (1997).
[36] I. P. Omelyan, I. M. Mryglod, and M. V. Tokarchuk, Phys. Rev. E **57**, 6667 (1998).
[37] S. Banerjee, R. B. Griffiths, and M. Widom, J. Stat. Phys. **93**, 109 (1998).
[38] P. J. Camp, J. C. Shelly, and G. N. Patey, Phys. Rev. Lett. **84**, 115 (2000).
[39] J. L. McWhirter and G. N. Patey, J. Chem. Phys. **117**, 9016 (2002).
[40] S. Varga, I. Szalai, J. Liszi, and G. Jackson, J. Chem. Phys. **116**, 9107 (2002).
[41] V. V. Murashov, P. J. Camp, and G. N. Patey, J. Chem. Phys. **116**, 6731 (2002).
[42] S. H. L. Klapp and M. Schoen, J. Chem. Phys. **117**, 8050 (2002).
[43] G. N. Chuev, M. V. Fedorov, and N. Russo, Phys. Rev. B **67**, 125103 (2003).
[44] V. Ballenegger and J.-P. Hansen, Mol. Phys. **102**, 599 (2004).
[45] B. E. Vugmeister and M. D. Glinchuk, Rev. Mod. Phys. **62**, 993 (1990).
[46] I. I. Naumov, L. Bellaiche, and H. Fu, Nature (London) **432**, 737 (2004).
[47] J. Higo, M. Sasai, H. Shirai, H. Nakamura, and T. Kugimiya, Proc. Natl. Acad. Sci. U.S.A. **98**, 5961 (2001).